Interference effects on eccentric tall buildings

K.S. Wong, K.C.S. Kwok
Department of Civil Engineering, The Hong Kong University of Science and Technology, Hong Kong S.A.R., P.R. China
P.A. Hitchcock
CLP Power Wind/Wave Tunnel Facility, The Hong Kong University of Science and Technology, Hong Kong S.A.R., P.R. China

1. INTRODUCTION

Modern tall buildings are typically lightweight, lightly damped and slender. As well as being susceptible to wind-induced vibrations, modern designs often have complex geometrical shape and/or asymmetrical distributions of stiffness and mass. Thus, these buildings often have eccentricities between center of mass and center of stiffness. Thepmongkorn and Kwok (2002) conducted wind tunnel tests on an aeroelastic CAARC model with different degrees of eccentricity. They found that in addition to the typical lateral motions, eccentric tall buildings are likely to have significant torsional responses. As tall buildings are rarely isolated, the presence of nearby buildings may alter the flow patterns and the wind-induced responses of an interfered building may be amplified. Tang (2002) conducted a comprehensive wind tunnel tests on the interference effects using the CAARC standard tall building model and showed that both dynamic translational and torsional responses are generally increased due to interference effects.

This paper focuses on the results of the wind-induced interference effects on the CAARC standard tall building model with no eccentricity using the high-frequency base balance measurement technique. Buffeting factor contours of wind-induced responses have been obtained and the excitation mechanisms of critical locations are determined. Some preliminary results of the building model with eccentricity of 10% of building dimensions are presented as well.

2. EXPERIMENTAL CONFIGURATION

2.1. Wind tunnel and wind model

Wind tunnel tests on the CAARC standard tall building were conducted in the high-speed section of the boundary layer wind tunnel of the CLP Power Wind/Wave Tunnel Facility at The Hong Kong University of Science and Technology.

For this study, the approach wind was modeled as terrain category 2 in AS/NZS1170.2:2002 as shown in Figure 1. The turbulence intensity at the top of the building model is about 0.1.

2.2. Tall building model

The CAARC standard tall building was modeled at 1:400 scale and used for both the principal and interfering buildings. The physical dimensions of the prototype building are $b = 45m$, $d = 30m$ and $h = 180m$ with structural density $\rho_s = 160kg/m^3$. The building is flat-topped, without parapets, and the exterior walls are flat and without any geometrical disturbance.

Only the fundamental mode of vibration will be considered for the determination of the wind-induced responses. The building was assumed to have linear mode shapes in translation and a constant torsional mode shape. Structural damping was assumed to be 1% of critical for all modes of vibration.

The natural frequencies of the fundamental translational modes were taken as 0.2 Hz. The prototype building was assumed to have a translational-torsional frequency ratio of 1.5. This implies that the torsional natural frequency is 0.3 Hz.

2.3. Incident wind velocity

Wind-induced responses were determined for a reduced wind velocity, $U_r = U(H)/n_1 b$, of 6. In which n_1 is the natural frequency of the fundamental translational mode of the prototype, and b is the breadth of the prototype.

2.4. Experiment method

The high-frequency base balance technique was used to measure directly the force and moment spectra to determine the lateral and torsional responses of the building.

Two 1:400 scale CAARC standard tall building were used as both the principal and interfering building in the test, as shown in Figure 2(a). The center of geometry of the interfering building was located according to the coordinate system as shown in Figure 2(b). The closest interfering building location was 1.5b and 1.5d from the center of geometry of the principal building and the furthest location was 10d upstream, 4d downstream and 4b laterally.

3. RESULTS

3.1. Building with no eccentricity

Buffeting factors, as defined in Equation (1), were used to quantify interference effects.

$$\mathrm{BF} = \frac{\text{Interfered building response}}{\text{Isolated building response}} \quad (1)$$

The buffeting factor contours of mean and standard deviation along-wind displacement, standard deviation cross-wind displacement and standard deviation twist angle are plotted in Figure 3.

As shown in Figure 3(a), the mean along wind displacement decreased when the interfering building was located upstream of the principal building and is due to the shielding effect of the upstream interfering building. Negative buffeting factors were found in the region from 1.5d to 3d. In this location, the principal building is submerged in the wake of the interfering building,

In Figure 3(b), the standard deviation along-wind response was generally increased when the interfering building was located upstream of the principal building. A critical buffeting factor of 1.37 has been found at (X, Y) = (7d, 1b). The along wind force spectrum in Figure 4 shows that the excitation energies at reduced frequencies greater than 0.1 are substantially increased. A peak near the reduced frequency of 0.1 corresponds to the vortex shedding frequency of the upstream interfering building. These enhanced energies are attributed to the well-organized incident vortices near the edge of the wake of the upstream building.

The standard deviation cross-wind

displacement buffeting factor contours demonstrate that the cross-wind response is enhanced when the interfering building is located upstream of the principal building. At (X, Y) = (7d, 2b), the standard deviation cross-wind displacement increased by almost 50%. The corresponding force spectrum in Figure 5 (a) shows increased energy over the whole spectrum. This indicates that the incident turbulence near the edge of the wake of the interfering building is intensified.

With the interfering building located at (X, Y) = (0, 3b), (-2d, 2b) and (-3d, 1b), the buffeting factors were 1.26, 1.45 and 1.26 respectively. Similar characteristics were found in the force spectra of these interfering cases, as shown in Figure 5 (b) – (d) respectively. The energy peak at the reduced frequency of 0.1 due to the wake excitation has been shifted to a high reduced frequency side. It seems that the interfering building altered the formation of the wake behind the principal building, thus increased the excitation energy near the natural frequency of the cross-wind mode. As a result, the cross-wind displacement response was amplified.

Substantial increases in standard deviation twist angle response were found when the interfering building was located at (X, Y) = (8d, 3b). The normalized torque spectrum in Figure 6(a) shows a general increase in energy. The enhanced energies appear to be the result of the intensified incident turbulence induced by the interfering building. Thus the standard deviation twist angle response is increased by approximately 50%.

When the interfering building is located at (X, Y) = (3d, 0), the standard deviation twist angle response is increased by almost 80%. In Figure 6(b), it can be seen that the energy is increased above a reduced frequency of 0.1 and is probably a result of the principal building being submerged in the highly turbulent wake of the interfering building. The increased energy close to the natural frequency of the torsional mode enhances the standard deviation twist angle response of the building.

For the interfering building located at (X, Y) = (-2d, 1b), the normalized torque spectrum in Figure 6 (c) shows that the energy peak at the reduced frequency of 0.1 is suppressed whereas the energy at the higher reduced frequencies are slightly increased. Similar to downstream interference effects on cross-wind response, the presence of downstream interfering building altered the flow around the principal building and formation of wake. Redistribution of excitation energy to the natural frequency of torsional mode cause about 30% increase in standard deviation twist angle response.

3.2. Building with 10% eccentricity

10% of eccentricity has been modelled by physically offsetting the center of stiffness. The translational moment spectra were found to be essentially unchanged. The buffeting factor of critical interfering cases found in buffeting factor contour of standard deviation twist angle is presented. The buffeting factors of standard deviation twist angle and the amplifications of standard deviation twist angle response of isolated building and 2 eccentric cases, as shown in Figure 7, have been summarized in Table 1. It can be seen that the standard deviation twist angle response amplification factor of isolated building of Case 1 is smaller than 1. On the contrary, that of isolated building of Case 2 is greater than 1. This implies that the standard deviation twist angle response would be affected by the eccentricity of the model.

Similarly, the buffeting factors of each eccentricity cases at particular interfering location are different. Besides the buffeting factors, the normalized torque spectra of each eccentric case, as shown in Figure 8 and 9, at particular interfering locations are different too. This implies that the excitation mechanism changes significantly according to the eccentricity between center of mass and center of stiffness.

4. CONCLUSIONS

The interference effects on CAARC standard tall building with no eccentricity by using high frequency base balance. The excitation mechanism can also been determined by direct measurement of force spectra.

Interference effects on eccentric building model are expected to be different from that on building model with no eccentricity in terms of excitation mechanisms and buffeting factors. The interference effects on eccentric tall building are currently being investigated in detail.

5. ACKNOWLEDGEMENTS

This research project is funded by a Research Grants Council of Hong Kong Central Allocation Grant (Project CA02/03.EG03) and a HKUST High Impact Areas Grant (HIA02/03.EG01). Thanks also go to the staff of the CLP Power Wind/Wave Tunnel Facility at HKUST.

6. REFERENCES

1. W.H. Melbourne, Comparison of measurements on the CAARC standard tall building model in simulated model wind flows, J. Wind Eng. Ind. Aerodyn. 6 (1980) 73 – 88.
2. S. Thepmongkorn, K.C.S. Kwok, Wind-induced responses of tall buildings experiencing complex motion, J. Wind Eng. Ind. Aerodyn. 90 (2002) 515 – 526.
3. U.F. Tang, Interference effects of wind-excited tall buildings, M.Phil Thesis, Department of Civil Engineering, HKUST, Hong Kong.

Cases	Amplification of isolated building	Buffeting factors (X, Y) = (3d, 0)	Buffeting factors (X, Y) = (-2d, 1)
0	1	1.79	1.31
1	0.79	2.4	1.37
2	1.17	1.37	1.34

Table 1 Amplification factors and buffeting factors

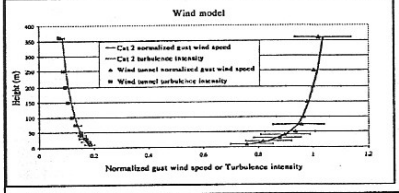

Figure 1 Wind model of terrain category 2 in AS/NZS 1170.2:2002

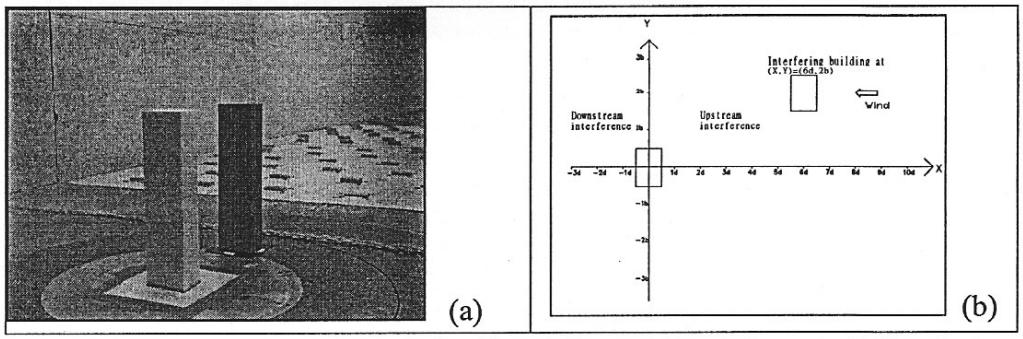

Figure 2 CAARC model: (a) Principal and interfering model in wind tunnel; (b) Coordinate system for interfering building

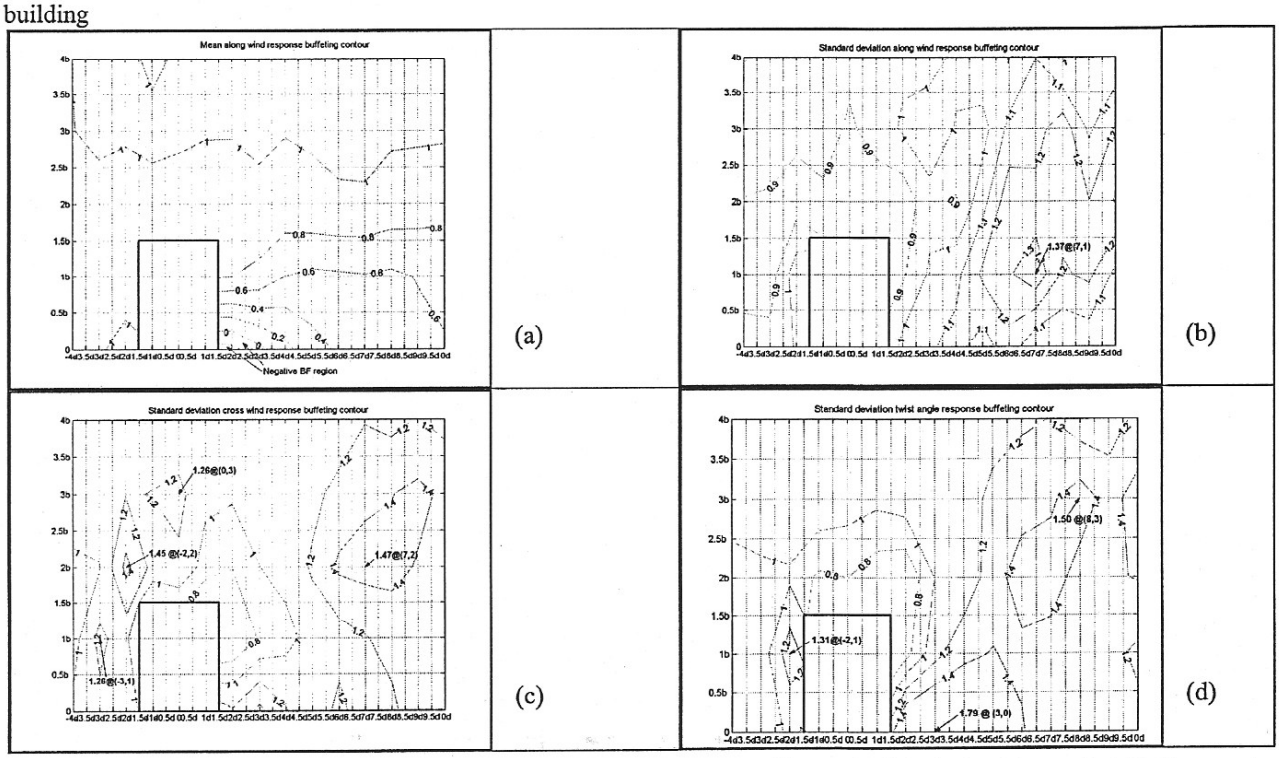

Figure 3 Buffeting factor contours: (a) mean along-wind displacement; (b) standard deviation along-wind displacement; (c) standard deviation cross wind displacement (d) standard deviation twist angle response.

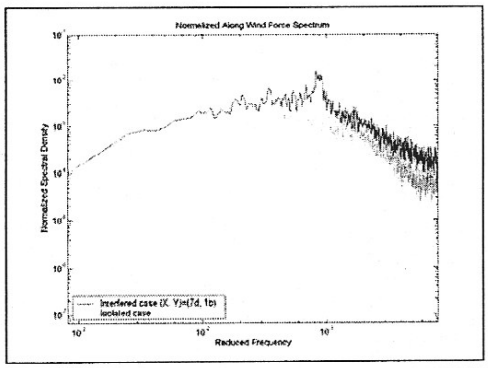

Figure 4 Along wind force spectrum (X, Y) = (7d, 1b)

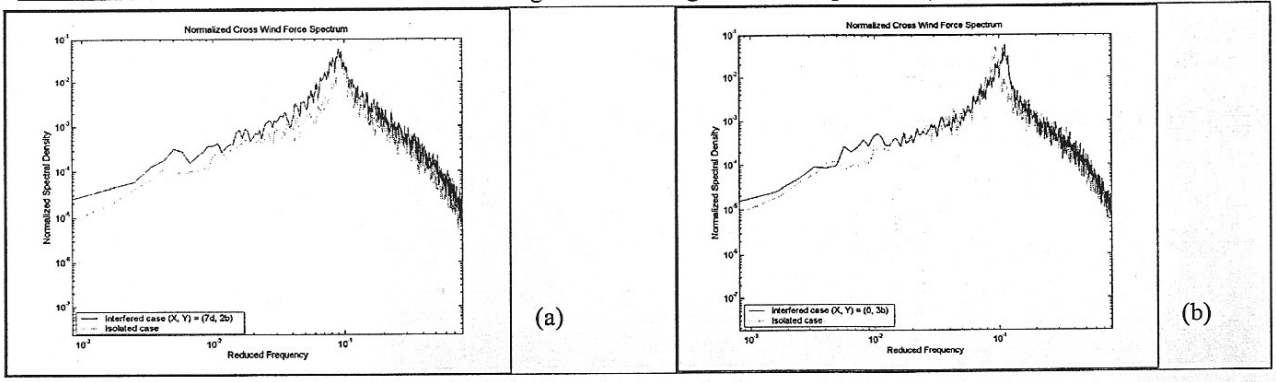

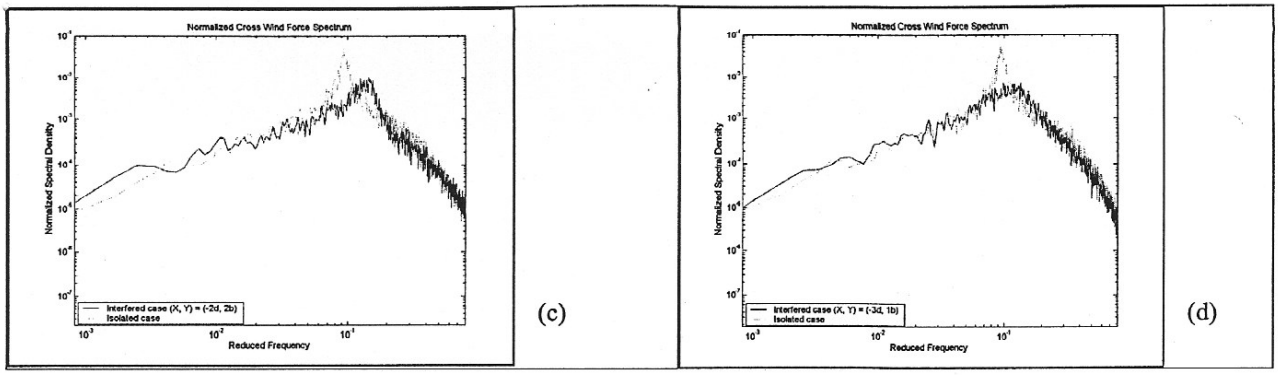

Figure 5 The normalized cross-wind force spectra of interfering cases: (a) (X, Y) = (7d, 2b); (b) (X, Y) = (0, 3b); (c) (X, Y) = (-2d, 2b); (d) (X, Y) = (-3d, 1b)

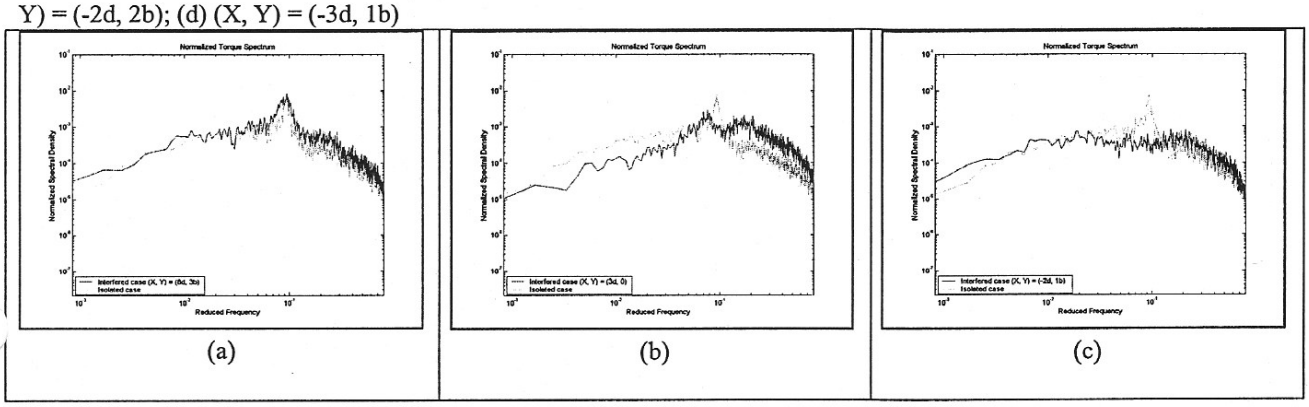

Figure 6 The normalized torque spectra of interfering cases: (a) (X, Y)=(8d, 3b); (b) (X, Y)=(3d, 0); (c) (X, Y)=(-2d, 1b)

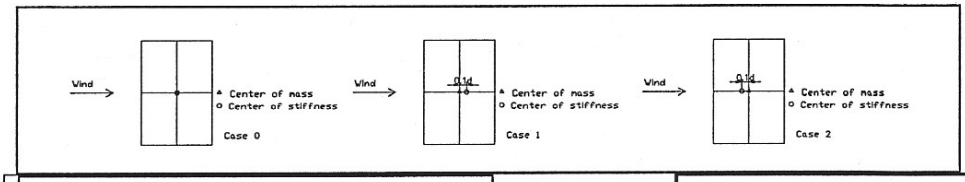

Figure 7 Eccentric model arrangement

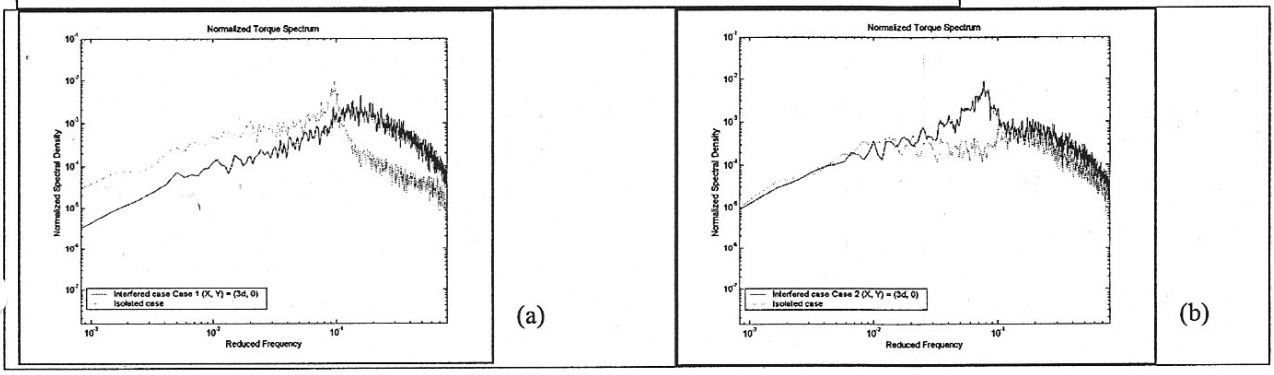

Figure 8 The normalized torque spectra of interfering building located at (X, Y)=(3d, 0): (a)Case 1; (b)Case 2

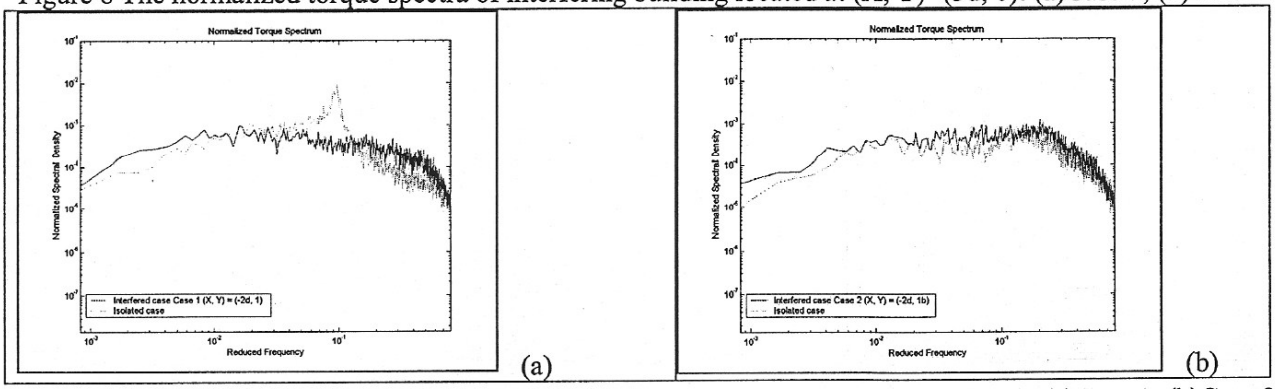

Figure 9 The normalized torque spectra of interfering building located at (X, Y)=(-2d, 1): (a)Case 1; (b)Case 2